Supplementary Material

PRPF19 mediates the proteasomal degradation of VDR to exacerbate ferroptosis in diabetic nephropathy

Qiongyao He[1,5], Wu He[2], Yanlin Ren[3], Wenbin Wu[1], Hui Dong[4], Gang Yuan[5], Huihui Ren[5], Xinwei Wang[6], Fuer Lu[4*], Dingkun Wang [4*]

[1]*Institute of Integrated Traditional Chinese and Western Medicine, Tongji Hospital, Tongji Medical College, Huazhong University of Science and Technology, Wuhan 430030, China*

[2]*Division of Cardiology, Department of Internal Medicine and Hubei Key Laboratory of Genetics and Molecular Mechanism of Cardiologic Disorders, Tongji Hospital, Tongji Medical College, Huazhong University of Science and Technology, Wuhan, 430000, China*

[3]*Department of Traditional Chinese Medicine, Zhongshan Hospital of Hubei Province, Wuhan 430030, China*

[4]*Department of Integrated Traditional Chinese and Western Medicine, Tongji Medical College, Tongji Hospital, Huazhong University of Science and Technology, Wuhan 430030, China*

[5]*Department of Endocrinology, Department of Internal Medicine, Tongji Hospital, Tongji Medical College, Huazhong University of Science and Technology, Wuhan 430030, China*

[6]*College of Pharmacy, Hubei University of Chinese Medicine, Wuhan 430065, China*

***To whom correspondence should be addressed:**

Dr Fuer Lu, Department of Integrated Traditional Chinese and Western Medicine, Tongji Medical College, Tongji Hospital, Huazhong University of Science and Technology, Wuhan 430030, China**,** Email: felutjh88@163.com

Dr Dingkun Wang, Department of Integrated Traditional Chinese and Western Medicine, Tongji Medical College, Tongji Hospital, Huazhong University of Science and Technology, Wuhan 430030, China**,** Email: wdkung@163.com;

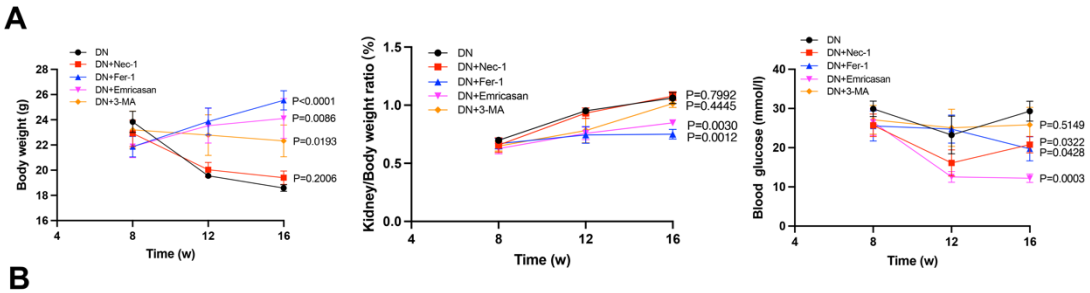
A
DN
DN+Nec-1
DN+Fer-1
DN+Emricasan
DN+3-MA
Body weight (g)
Time (w)
P<0.0001
P=0.0086
P=0.0193
P=0.2006
Kidney/Body weight ratio (%)
P=0.7992
P=0.4445
P=0.0030
P=0.0012
Blood glucose (mmol/l)
P=0.5149
P=0.0322
P=0.0428
P=0.0003

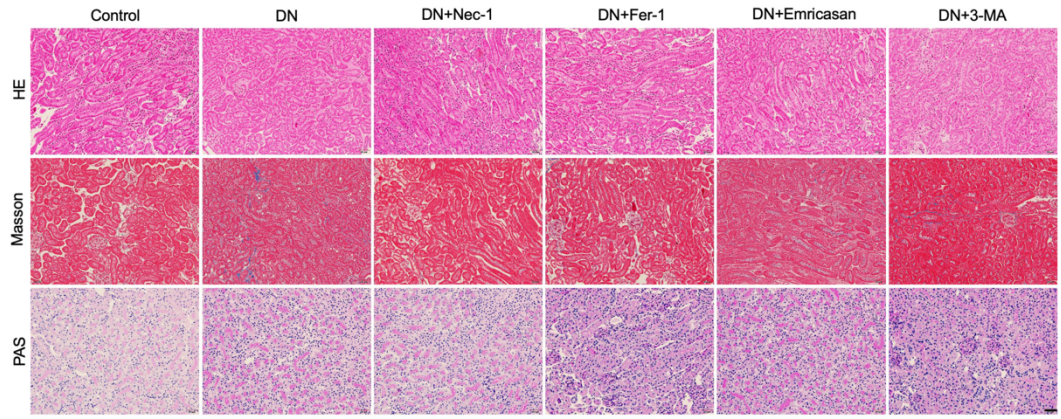
B
Control
DN
DN+Nec-1
DN+Fer-1
DN+Emricasan
DN+3-MA
HE
Masson
PAS

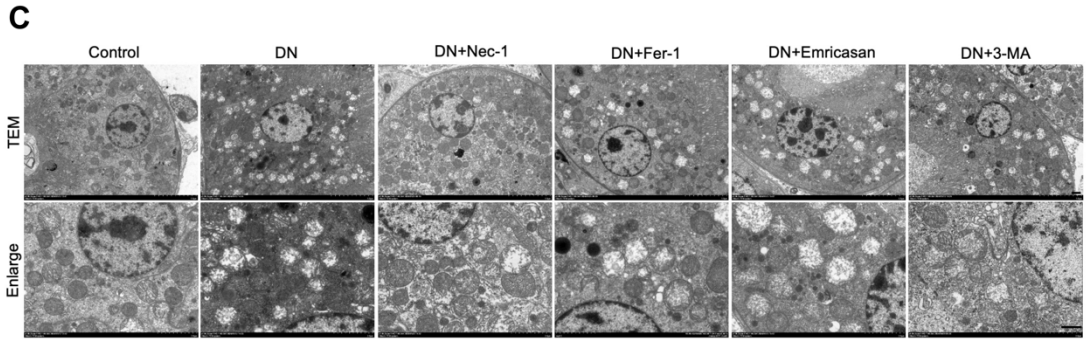
C
Control
DN
DN+Nec-1
DN+Fer-1
DN+Emricasan
DN+3-MA
TEM
Enlarge

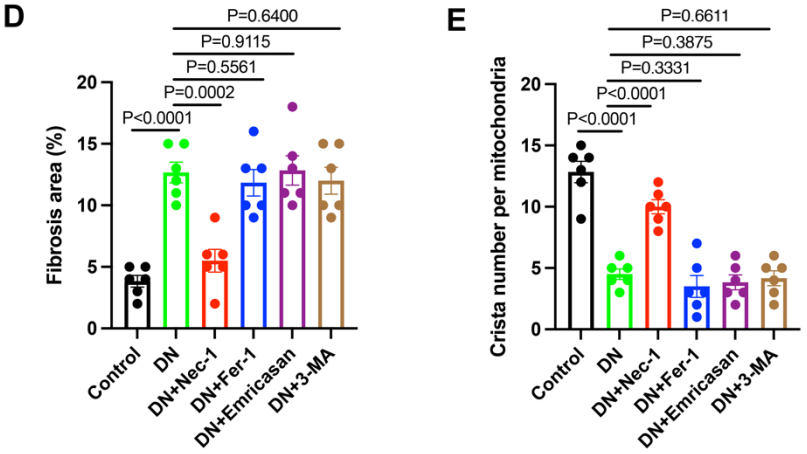
D
Fibrosis area (%)
P=0.6400
P=0.9115
P=0.5561
P=0.0002
P<0.0001
Control
DN
DN+Nec-1
DN+Fer-1
DN+Emricasan
DN+3-MA

E
Crista number per mitochondria
P=0.6611
P=0.3875
P=0.3331
P<0.0001
P<0.0001
Control
DN
DN+Nec-1
DN+Fer-1
DN+Emricasan
DN+3-MA

32
33

Fig S1. Necrosis is the predominant form of cell death in the early-stage of DN.

(A) Levels of body weight, kidney/body weight ratio and blood glucose in DN mice treated with Nec-1 (5 mg·kg-1·d-1), Fer-1 (5 mg·kg-1·d-1), Emricasan (12.5 mg·kg-1·d-1), 3-MA (10 mg·kg-1·d-1), or vehicle (n = 5 or 6). (B) H&E, Masson and PAS staining of kidney sections collected from mice in the indicated groups at week 8 (bar = 100 μm). (C) Representative transmission electron microscopy images of PTECs from mice in the indicated groups at week 8 (bar = 10 μm). (D) Quantification of tubulointerstitial fibrosis in the kidney cortex at week 8. (E) Absolute counting of the number of cristae per mitochondria at week 8. Data are expressed as means ± SEM. Student's t-test was employed for comparisons between two groups; one-way ANOVA followed by Tukey's post-test for multiple comparisons was used for groups of three or more.

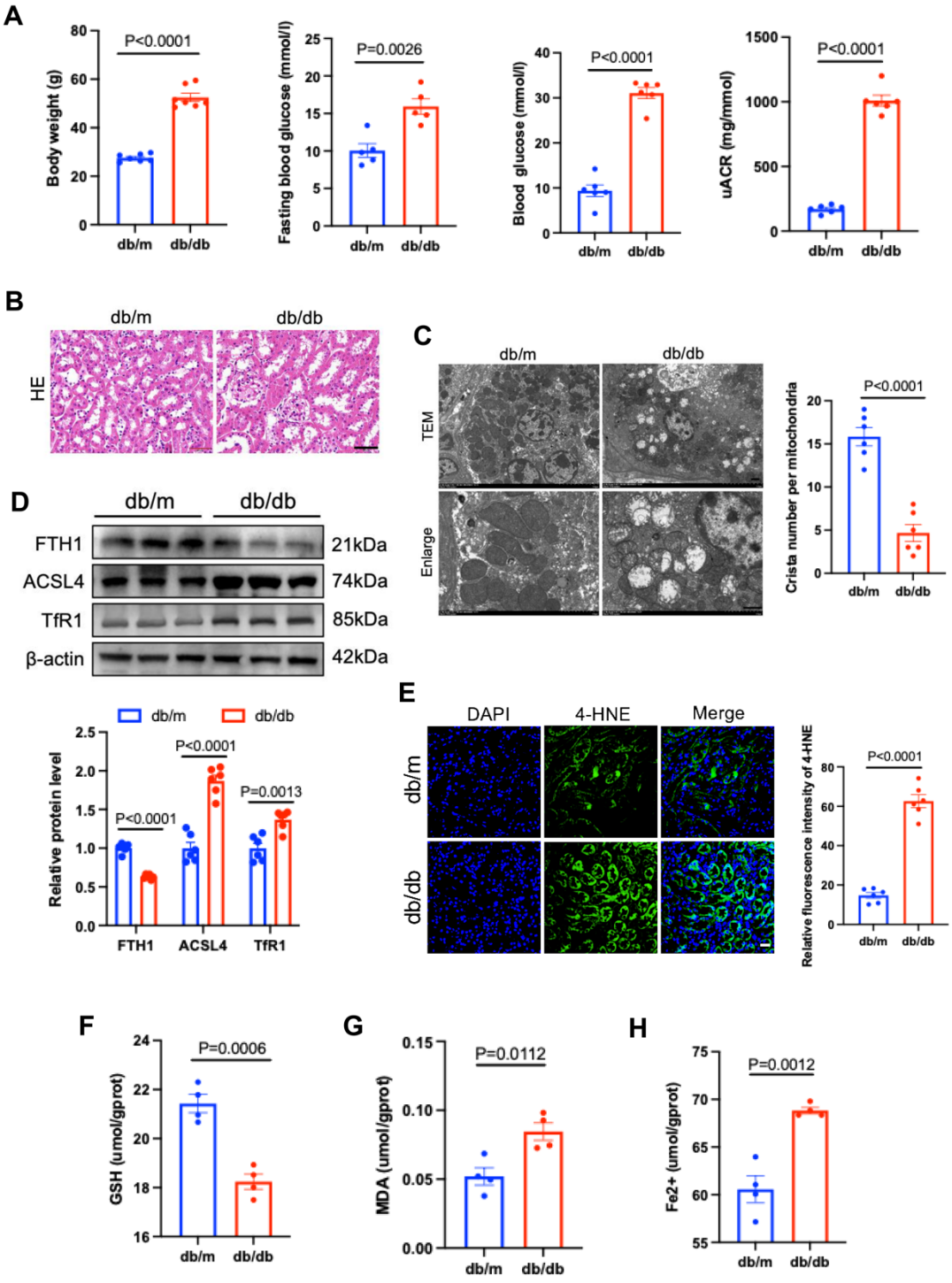
A
Body weight (g)
P<0.0001
db/m
db/db
Fasting blood glucose (mmol/l)
P=0.0026
Blood glucose (mmol/l)
P<0.0001
uACR (mg/mmol)
P<0.0001
B
HE
C
TEM
Enlarge
Crista number per mitochondria
P<0.0001
D
FTH1
ACSL4
TfR1
β-actin
21kDa
74kDa
85kDa
42kDa
Relative protein level
P<0.0001
P=0.0013
E
DAPI
4-HNE
Merge
Relative fluorescence intensity of 4-HNE
F
GSH (umol/gprot)
P=0.0006
G
MDA (umol/gprot)
P=0.0112
H
Fe2+ (umol/gprot)
P=0.0012

Fig S2. Ferroptosis in renal tubular cells of db/db mice.

(A) Levels of body weight, fasting blood glucose, blood glucose and uACR in db/db or db/m mice (n = 5-7). (B) H&E staining of kidney sections collected from db/db or db/m mice (bar = 50 μm). (C) Representative transmission electron microscopy images of PTECs from db/db or db/m mice (bar = 10 μm). (D) Western blotting of FTH1, ACSL4 and TfR1 in the kidney tissues of db/db or db/m mice (n = 6). (E) Immunofluorescence staining of 4-HNE of PTECs from db/db or db/m mice (n = 6; bar = 50 μm). (F-H) GSH, MDA and iron levels of db/db or db/m mice (n = 4). Data are expressed as means ± SEM. Student's t-test was employed for comparisons between two groups; one-way ANOVA followed by Tukey's post-test for multiple comparisons was used for groups of three or more.

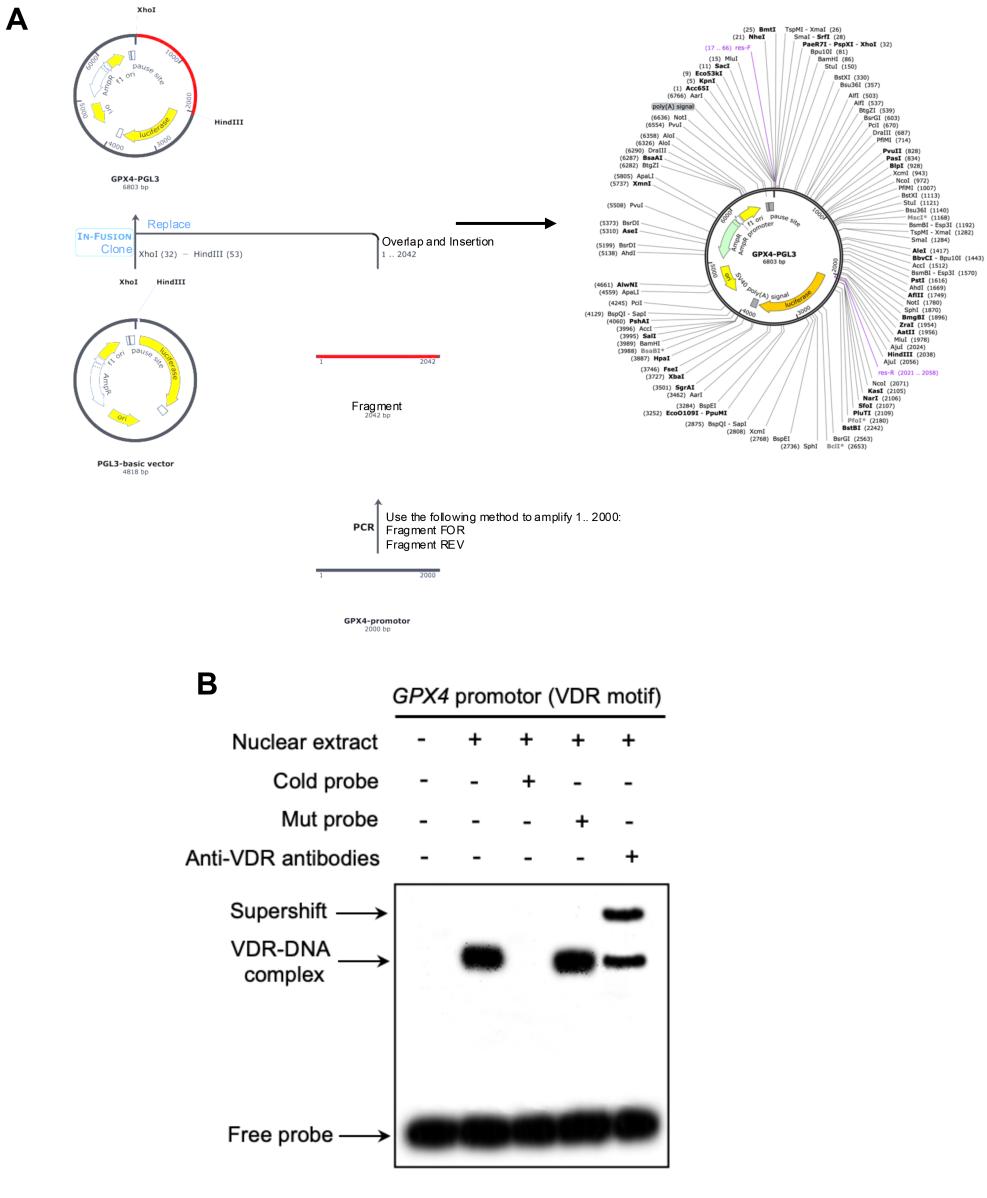

Fig S3. VDR is a key transcriptional regulator of GPX4.

(A) Schematic diagram of synthesis of PGL3-GPX4 luc plasmid. (B) Nuclear extracts from HK-2 cells were incubated with anti-VDR antibodies for 15min prior to further incubating with biotin-labeled probes containing VDR motif from GPX4 promoter. The VDR-DNA complexes and supershifts were measured using EMSA.

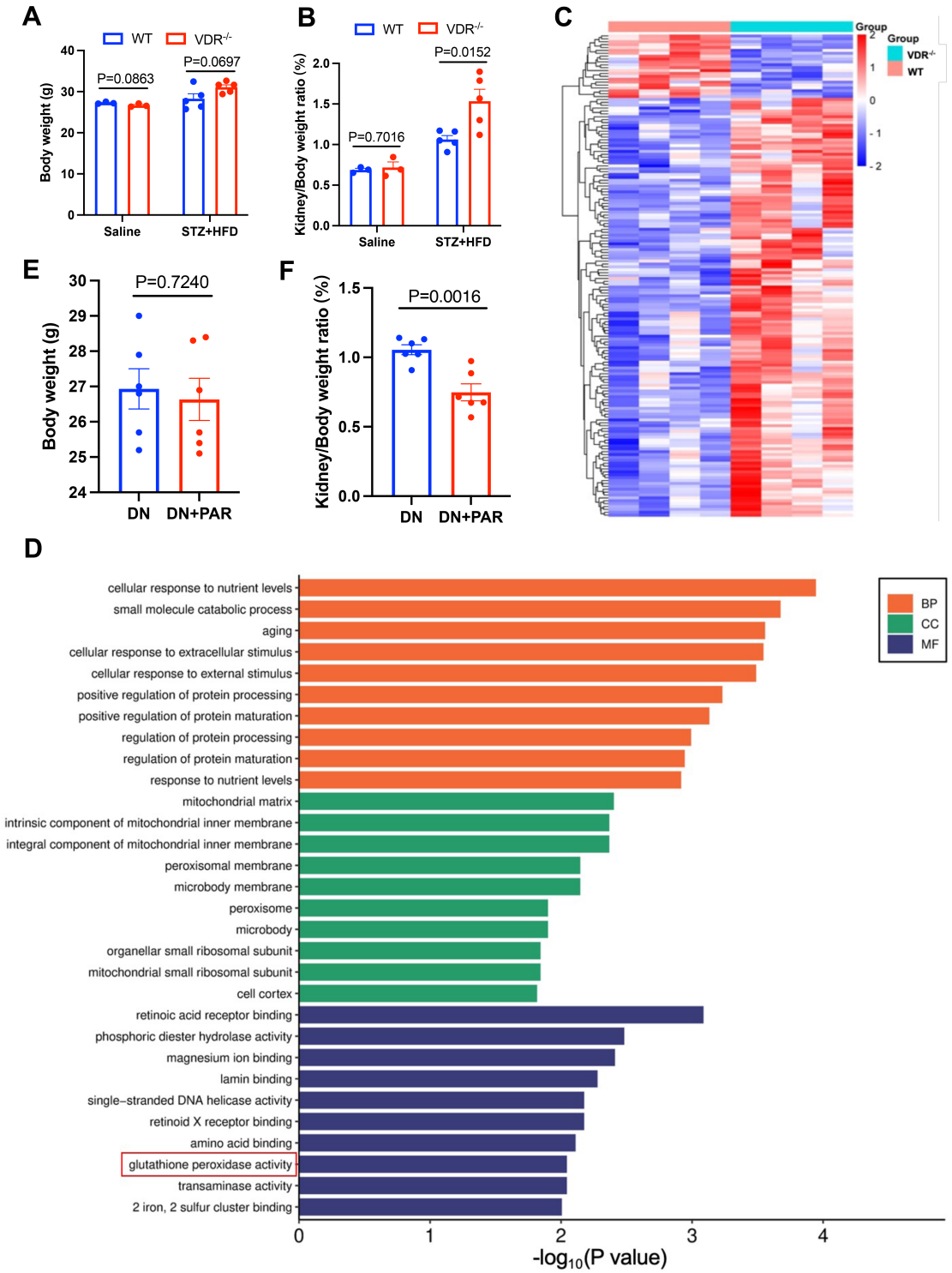
A
WT
VDR-/-
P=0.0863
P=0.0697
Body weight (g)
Saline
STZ+HFD
B
WT
VDR-/-
P=0.7016
P=0.0152
Kidney/Body weight ratio (%)
Saline
STZ+HFD
C
Group
VDR-/-
WT
E
P=0.7240
Body weight (g)
DN
DN+PAR
F
P=0.0016
Kidney/Body weight ratio (%)
DN
DN+PAR
D
BP
CC
MF
cellular response to nutrient levels
small molecule catabolic process
aging
cellular response to extracellular stimulus
cellular response to external stimulus
positive regulation of protein processing
positive regulation of protein maturation
regulation of protein processing
regulation of protein maturation
response to nutrient levels
mitochondrial matrix
intrinsic component of mitochondrial inner membrane
integral component of mitochondrial inner membrane
peroxisomal membrane
microbody membrane
peroxisome
microbody
organellar small ribosomal subunit
mitochondrial small ribosomal subunit
cell cortex
retinoic acid receptor binding
phosphoric diester hydrolase activity
magnesium ion binding
lamin binding
single−stranded DNA helicase activity
retinoid X receptor binding
amino acid binding
glutathione peroxidase activity
transaminase activity
2 iron, 2 sulfur cluster binding
-log10(P value)

Fig S4. VDR deletion promotes ferroptosis to exacerbate renal tubule injury in DN mice.

(A and B) Levels of body weight and kidney/body weight ratio in mice in the indicated groups (n = 3/5). (C) Heatmap showing the expression of differential genes in the kidney tissues of $VDR^{-/-}$ and WT mice treated with STZ and HFD (n = 3). (D) GO enrichment analysis of differentially expressed genes in $VDR^{-/-}$ and WT mice treated with STZ and HFD. (E and F) Levels of body weight and kidney/body weight ratio in DN mice treated with PAR or vehicle (n = 6). Data are expressed as means ± SEM. Student's t-test was employed for comparisons between two groups; one-way ANOVA followed by Tukey's post-test for multiple comparisons was used for groups of three or more.

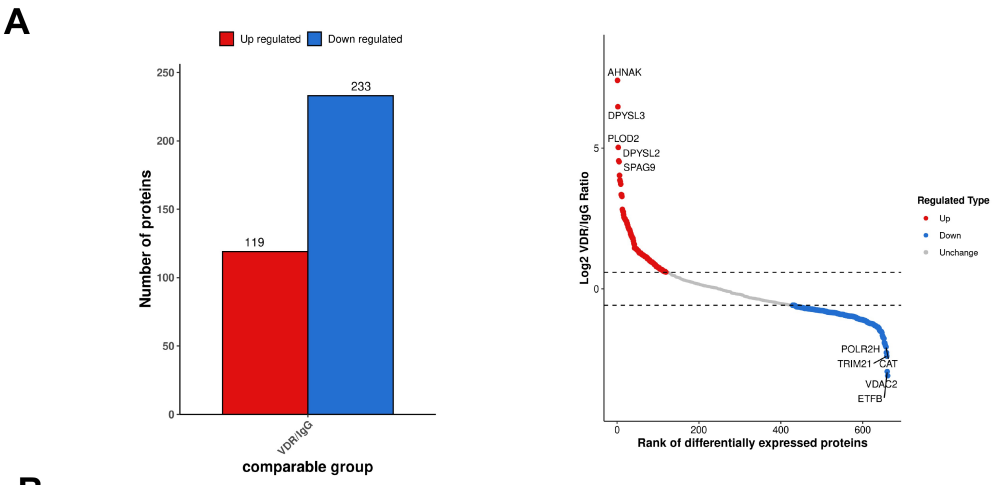
A
Up regulated
Down regulated
Number of proteins
250
200
150
100
50
0
233
119
VDR/IgG
comparable group
AHNAK
DPYSL3
PLOD2
DPYSL2
SPAG9
POLR2H
TRIM21
CAT
VDAC2
ETFB
Log2 VDR/IgG Ratio
5
0
0
200
400
600
Rank of differentially expressed proteins
Regulated Type
Up
Down
Unchange

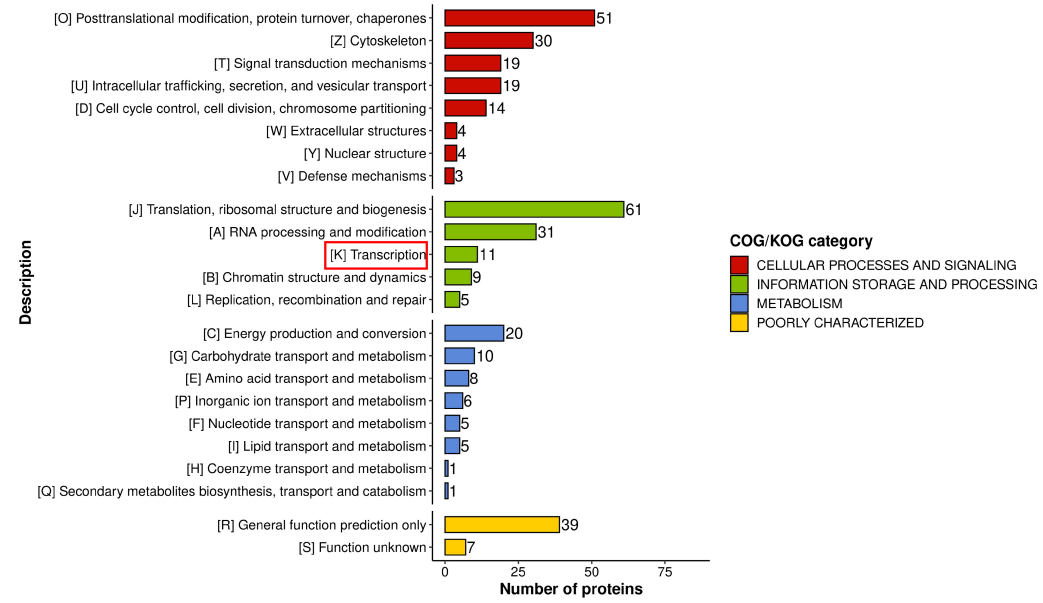
B
[O] Posttranslational modification, protein turnover, chaperones
[Z] Cytoskeleton
[T] Signal transduction mechanisms
[U] Intracellular trafficking, secretion, and vesicular transport
[D] Cell cycle control, cell division, chromosome partitioning
[W] Extracellular structures
[Y] Nuclear structure
[V] Defense mechanisms
[J] Translation, ribosomal structure and biogenesis
[A] RNA processing and modification
[K] Transcription
[B] Chromatin structure and dynamics
[L] Replication, recombination and repair
[C] Energy production and conversion
[G] Carbohydrate transport and metabolism
[E] Amino acid transport and metabolism
[P] Inorganic ion transport and metabolism
[F] Nucleotide transport and metabolism
[I] Lipid transport and metabolism
[H] Coenzyme transport and metabolism
[Q] Secondary metabolites biosynthesis, transport and catabolism
[R] General function prediction only
[S] Function unknown
51
30
19
19
14
4
4
3
61
31
11
9
5
20
10
8
6
5
5
1
1
39
7
Description
0
25
50
75
Number of proteins
COG/KOG category
CELLULAR PROCESSES AND SIGNALING
INFORMATION STORAGE AND PROCESSING
METABOLISM
POORLY CHARACTERIZED

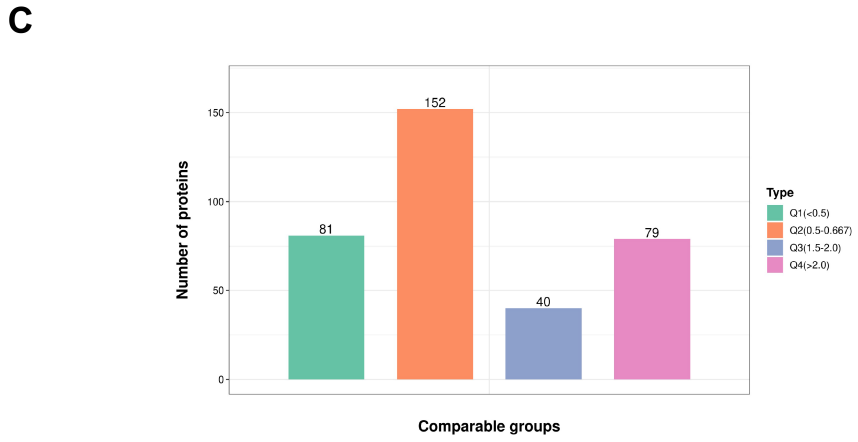
C
Number of proteins
150
100
50
0
81
152
40
79
Comparable groups
Type
Q1(<0.5)
Q2(0.5-0.667)
Q3(1.5-2.0)
Q4(>2.0)

84

85

Fig S5. E3 ubiquitin ligase PRPF19 mediates ubiquitination degradation of VDR. (A) Statistical and scatter plots of differential proteins. (B) Perform COG/KOG classification analysis on the selected differentially expressed proteins. (C) In order to compare the functional similarities and differences between proteins with different expression levels, we divided the proteins into four parts, called Q1 to Q4, based on their differential expression levels, and performed GO, KEGG enrichment, and COG/KOG category analysis on each part.

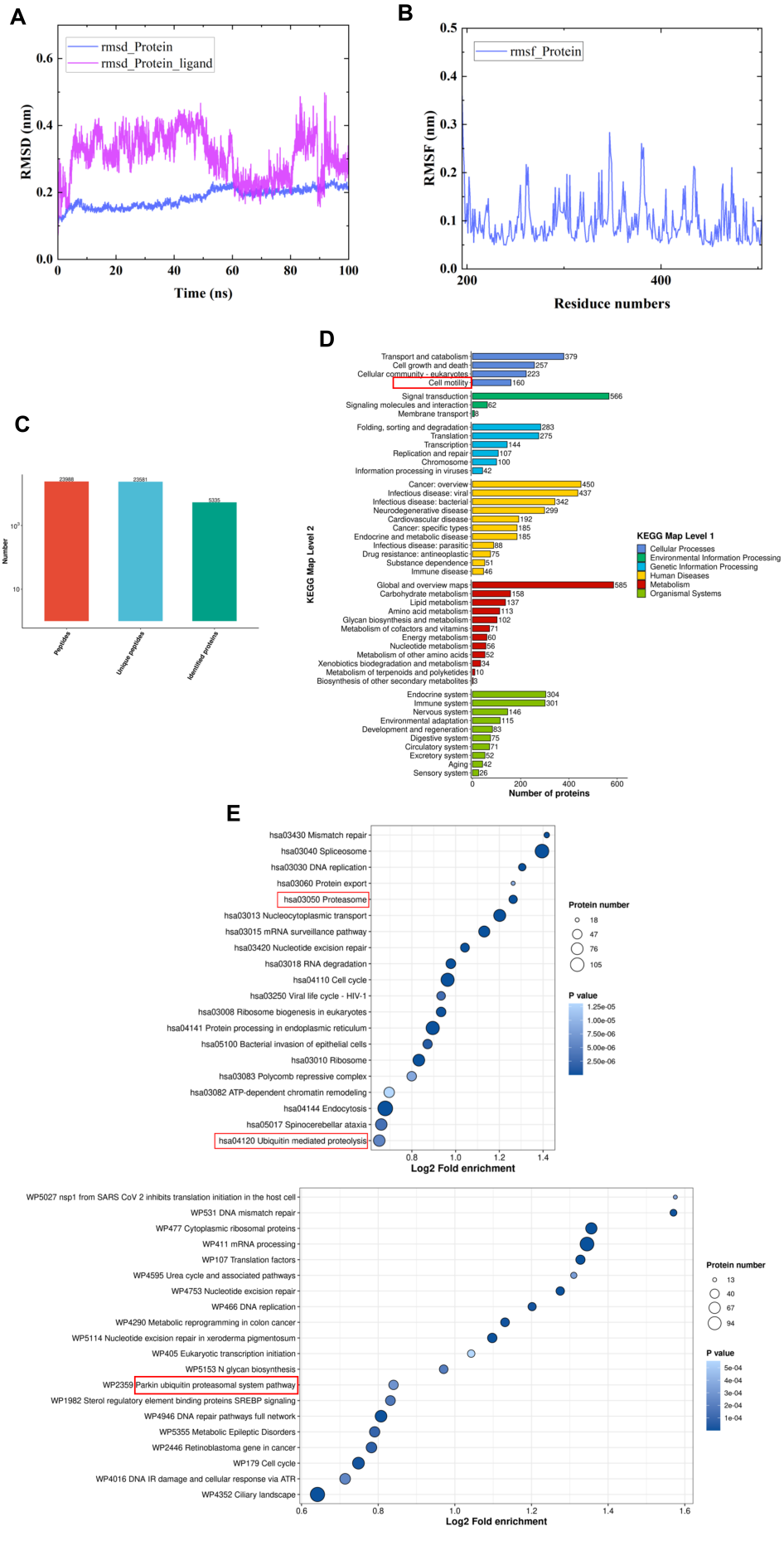
A
rmsd_Protein
rmsd_Protein_ligand
RMSD (nm)
Time (ns)
B
rmsf_Protein
RMSF (nm)
Residuce numbers
C
Number
Peptides
Unique peptides
Identified proteins
D
KEGG Map Level 2
Number of proteins
KEGG Map Level 1
Cellular Processes
Environmental Information Processing
Genetic Information Processing
Human Diseases
Metabolism
Organismal Systems
E
Protein number
P value
Log2 Fold enrichment

Fig S6. BBR and VDR competitively bind to PRPF19.

(A) The plots of RMSD of BBR-PRPF19 complex and free PRFP19. (B) The plots of RMSF of BBR-PRPF19 complex. (C) The overall situation of peptide segments and protein numbers identified in protein group. (D) Perform KEGG pathway classification analysis on identified proteins. (E) Perform WikiPathways pathway enrichment analysis on identified proteins (up), and KEGG pathway analysis of BBR interacting proteins (down).

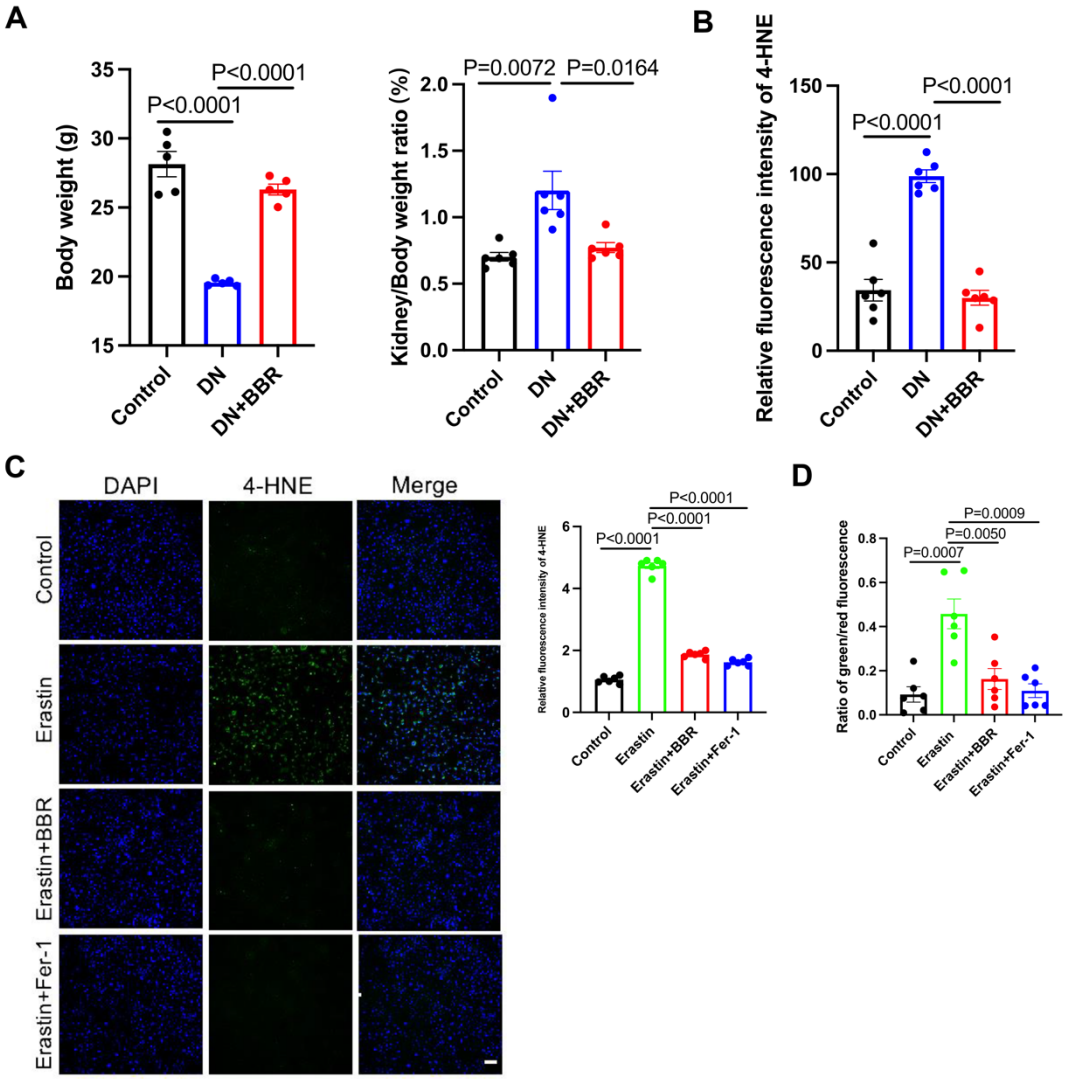

Fig S7. BBR inhibits ferroptosis of RTECs in vitro and in vivo.

(A) Levels of body weight and kidney/body weight ratio in DN mice treated with BBR or vehicle for 4 weeks (bar = 5 cm). (B) Analysis results of fluorescence staining of 4-HNE in DN mice treated with BBR or vehicle for 4 weeks (n = 6). (C) Immunofluorescence staining of 4-HNE in HK-2 cells treated with erastin (5 μM), BBR (10 μM), Fer-1 (5 μM) or vehicle (n = 6; bar = 50 μm). Data are expressed as means ± SEM. Student's t-test was employed for comparisons between two groups; one-way ANOVA followed by Tukey's post-test for multiple comparisons was used for groups of three or more.

Supplementary Table 1. Clinical information of the subjects

Characteristics	Diabetic Nephropathy (*n*=40)	Non-Diabetic Nephropathy (*n*=40)	*p* value
Age (years)	57.38±8.14	43.76±8.02	0.0017*
Male (n, %)	29 (72.50%)	25 (52.50%)	0.1080#
SCr (μmol/L)	512.88±153.87	79±13.53	2e-5*
BUN (mmol/L)	18.16±7.24	4.40±3.38	0.0010*
GFR (ml/min)	23.10±18.07	97±6.74	1.3e-8*
Comorbidities/ Medical history			
Hypertension	38 (95%)	0	
Diabetes mellitus	40 (100%)	0	
Coronary disease	9 (22.50%)	0	
Neurologic	0	0	
Neoplasms (extra-renal)	0	0	

#Fisher's two-tailed test. *Unpaired two-tailed t-test. GFR: Glomerular filtration rate.

Supplementary Table 2. List of primers used for qRT-PCR

Gene names	Primer	Sequence (5' to 3')
Mouse *GPX4*	Forward	CTCCGGAGACTCCTCCTCAA
Mouse *GPX4*	Reversed	AGCGCAACATGATCACCTCA
Mouse *VDR*	Forward	CCGTCTGAGCCGCTTACTTA
Mouse *VDR*	Reversed	TATCGGGCATGCAGATCGAC
Mouse *GAPDH*	Forward	GAGAGTGTTTCCTCGTCCCG
Mouse *GAPDH*	Reversed	ATCCGTTCACACCGACCTTC
Human *VDR*-Motif 1	Forward	TCACACCTGTAATCCCAGCACTCT
Human *VDR*-Motif 1	Reversed	TACACGAGCGAGCCACCACA
Human *VDR*-Motif 2	Forward	GCTGAGGCTGGAGGATCACTTG
Human *VDR*-Motif 2	Reversed	GGACAACAGGCTCATCCACCAT
Human *VDR*-Motif 3	Forward	GGTGACAGACCAAGACTCCTCAA
Human *VDR*-Motif 3	Reversed	GGCAACAGAAACACTCATCTCATACTT
Human *VDR*-Motif 4	Forward	ACGCCTCTGTGCTGCATCTG
Human *VDR*-Motif 4	Reversed	GGATTACAGGTGTGAGCCACTCTAC
Human *VDR*-Motif 5	Forward	GCCCTGAGTCTGTCTCTGAAGAAATAC
Human *VDR*-Motif 5	Reversed	CAAAGTGCTGGGATTACAGGTGTGA
Human *YY1*-Motif 1	Forward	CGGGAGCAAAGCCATGTGAACA
Human *YY1*-Motif 1	Reversed	AGATGCAGCACAGAGGCGTCAT
Human *YY1*-Motif 2	Forward	GCGTGGTAGCACATGCCTGTA
Human *YY1*-Motif 2	Reversed	GGAACTGAGTCACCGTGATTGGA
Human *YY1*-Motif 3	Forward	TGTCTTGATGACTCTCAGGTCTCAG
Human *YY1*-Motif 3	Reversed	GAGTGCTGGGATTACAGGTGTGA
Human *YY1*-Motif 4	Forward	TCGCAAGGGCAAGAACAGAGTC
Human *YY1*-Motif 4	Reversed	GCAGAGGCAGTGAAGCAAGGAT
Human *YY1*-Motif 5	Forward	TCTCAGGTCTCAGTGCCCACATTA
Human *YY1*-Motif 5	Reversed	TTGCTTCTCATCACAGCTCCATCTT
Human *POU2F2*-Motif 1	Forward	TCTCAGGTCTCAGTGCCCACAT
Human *POU2F2*-Motif 1	Reversed	GCCAGGCTGATCTCGAACTCCT

Human *POU2F2*-Motif 2	Forward	CTGTGATGAGAAGCAAACCCAACTC
Human *POU2F2*-Motif 2	Reversed	GGCTGATCTCGAACTCCTGACCT
Human *POU2F2*-Motif 3	Forward	TGAGTCAGGAGAATCGCTTGAACC
Human *POU2F2*-Motif 3	Reversed	GCTCATCCACCATTCCTGGCTAAT
Human *POU2F2*-Motif 4	Forward	AACCATCCATGACGCCTCTGTG
Human *POU2F2*-Motif 4	Reversed	TGGTCAGGCTGGTCTCGAACTC
Human *POU2F2*-Motif 5	Forward	AGAGACGGGAGGTTCGCTTGAG
Human *POU2F2*-Motif 5	Reversed	CGCAGTTATCCGGCTGGTTGAC

Supplementary Table 3. List of antibodies used in this study

Antibody	Source	Supplier	Catalog number
VDR	Rabbit	Abcam	ab109234
VDR	Mouse	Proteintech	67192-1-lg
GPX4	Mouse	Proteintech	67763-1-lg
PRPF19	Rabbit	Proteintech	15414-1-AP
FTH1	Rabbit	ABclonal	A19544
ACSL4	Rabbit	Proteintech	22401-1-AP
TfR1	Rabbit	ABclonal	A5865
4-HNE	Rabbit	Bioss	bs-6313R
YY1	Rabbit	Cell Signaling	46395S
POU2F2	Rabbit	BOSTER	M04407-2
Anti-MYC tag mAb	Rabbit	Proteintech	16286-1-AP
Anti-FLAG tag mAb	Mouse	Proteintech	66008-4-lg
Anti-Ubiquitin mAb	Mouse	ThermoFisher	13-1600
FITC Goat Anti-Rabbit IgG (H+L)	Goat	BOSTER	BA1032
FITC Goat Anti-Rabbit IgG (H+L)	Goat	ABclonal	AS011
CY3 Goat Anti-Rabbit IgG(H+L)	Goat	BOSTER	BA1105
β-actin	Mouse	Proteintech	66009-1-lg